24th INTERNATIONAL CONGRESS ON SOUND AND VIBRATION
23–27 July 2017, London

EFFECTS OF DEVIATIONS OF A MONKEY SKULL'S ACOUSTIC PARAMETERS ON TRANSCRANIAL FOCUSED ULTRASOUND

Chang Su, Weijun Lin, and Hanyin Cui

State Key Laboratory of Acoustics, Institute of Acoustics, Chinese Academy of Sciences, Beijing, 100190, China
email: suchang@mail.ioa.ac.cn

Xiangda Wang

State Key Laboratory of Acoustics, Institute of Acoustics, Chinese Academy of Sciences, Beijing, 100190, China
University of Chinese Academy of Sciences, Beijing 100049, China

For noninvasive transcranial focused ultrasound (tcFUS) applications, numerical simulations are necessary to assist corresponding experiments. And a precise simulation requires accurate acoustic parameters of a skull. However, completely accurate acquisition of the skull's acoustic parameters is difficult. Therefore, the investigation of how the skull's acoustic parameters may affect the transcranial focused ultrasonic field is important, as it helps to determine the deviation tolerance of the skull's acoustic parameters. In this paper, a 256-element planar phased array with the same emitting amplitude is used for transcranial focused ultrasound. The computed tomography (CT) scans of a monkey skull are used to reconstruct the three-dimensional (3D) skull model. The Kelvin-Voigt equation solved by the staggered-grid finite-difference-time-domain method is applied as the governing equation for transcranial focused ultrasound. The time-reversal method and the correlation technique are employed to help carry out phase modulations based on the 3D skull models with the hypothetically precise acoustic parameters and those deviating from the hypothetically precise ones. Subsequently, transcranial focused ultrasound fields with different phase modulations obtained above are respectively simulated based on the hypothetically precise acoustic parameters of the skull, no matter through which acoustic parameters of the skull the phase modulation is obtained. Numerical results indicate that the focusing effect of transcranial focused ultrasound denoted by the acoustic pressure focusing gain and the focusing deviation is almost not influenced by the deviations of the monkey skull's density and acoustic absorption coefficient in the scope of the deviation studied. The major influence on the focusing effect is contributed by the deviation of the skull's sound velocity. And an absolute deviation percentage less than 5.0% from the standard sound velocity is suggested to control the absolute focusing deviation and the deviation percentage of the acoustic pressure focusing gain lower than 0.5mm and 1.0%, respectively.

Keywords: tcFUS, acoustic parameter, numerical simulation

1. Introduction

For noninvasive applications of transcranial focused ultrasound (tcFUS) in assisting the treatments of brain diseases, the skull inserted on the ultrasound propagation path is the primary obstacle. The skull is strongly heterogeneous in its acoustic parameters such as the density and the sound velocity, and thus bring serious phase aberrations to transcranial focused ultrasound, which will result in a poor focusing of ultrasound and an undesired tissue heating outside the focal region (especially around the

skull) [1][2]. Different methods have been developed to compensate the phase aberrations in order to help the achievement of precise focus control of transcranial focused ultrasound, thus instructing the experiments utilizing transcranial focused ultrasound [3]. To accurately calculate the phase aberrations for a good focusing effect, accurate numerical simulations are necessary, which requires precise acoustic parameters of the skull. In other words, acoustic parameters of the skull have a great influence on the success of compensating the phase aberrations correctly and afterwards the success of noninvasive transcranial focused ultrasound applications.

Experimental measurements combined with empirical formulas have been employed to provide the skull's acoustic parameters [4][5]. However, there still exist deviations of a skull's acoustic parameters and it's still a difficult task to obtain the absolutely precise acoustic parameters of a skull [4]. Therefore, we want to present an investigation into the effects of deviations of the skull's acoustic parameters on transcranial focused ultrasound in this paper. A set of a monkey skull's acoustic parameters, i.e. the 3D monkey skull model, calculated according to its computed tomography (CT) scans [5] from Shenzhen Institutes of Advanced Technology, Chinese Academy of Sciences is hypothetically considered to be absolutely precise. The Kelvin-Voigt equation [6] with consideration of the mode conversion between compressional waves and shear waves inside the skull solved by staggered-grid finite difference time domain (FDTD) method is adopted for simulations of the acoustic field. A 256-element planar ultrasonic phased array transducer is used and the time reversal method [7] is employed to achieve a precise focus control of transcranial ultrasound based on the hypothetically precise 3D monkey skull model. Then, the hypothetically precise set of the skull's acoustic parameters is respectively replaced by several sets of the skull's acoustic parameters with different deviations to discuss and analyse the effects of deviations of the skull's acoustic parameters on transcranial focused ultrasound.

2. Materials and methods

2.1 Basic equations

The Kelvin-Voigt equation [6] for the isotropic inhomogeneous viscoelastic media can better describe the propagation of transcranial ultrasound since it can be responsible for the mode conversion between compressional waves and shear waves inside the skull. The detailed expression with the Einstein notation is:

$$\begin{cases} \rho_0 \dfrac{\partial V_i}{\partial t} = \dfrac{\partial T_{ij}}{\partial x_j} \\ \dfrac{\partial T_{ij}}{\partial t} = \lambda \delta_{ij} \dfrac{\partial V_k}{\partial x_k} + \mu \left(\dfrac{\partial V_i}{\partial x_j} + \dfrac{\partial V_j}{\partial x_i} \right) + \chi \delta_{ij} \dfrac{\partial^2 V_k}{\partial x_k \partial t} + \eta \left(\dfrac{\partial^2 V_i}{\partial x_j \partial t} + \dfrac{\partial^2 V_j}{\partial x_i \partial t} \right) \end{cases}. \tag{1}$$

The subscripts i, j and k are Einstein notations. T_{ij} and V_i are the stress and the particle velocity, respectively. δ_{ij} equalizes 1 when $i = j$ and equalizes to 0 when $i \neq j$. λ and μ are Lame constants, which can be expressed by the density of the media (ρ_0), shear wave velocity (c_s) and compressional wave velocity (c_p) as:

$$\begin{cases} \mu = c_s^2 \rho \\ \lambda + 2\mu = c_p^2 \rho_0 \end{cases}. \tag{2}$$

χ and η are respectively the viscosity coefficients of compressional waves and shear waves, which are related with the compressional wave absorption coefficient (α_p) and the shear wave absorption coefficient (α_s).

$$\begin{cases} \alpha_p \approx \alpha_{0,p} \omega^2 \\ \alpha_s \approx \alpha_{0,s} \omega^2 \end{cases}. \tag{3}$$

$$\begin{cases} \alpha_{0,p} = \dfrac{\chi + 2\eta}{2\rho_0 c_p^3} \\ \alpha_{0,s} = \dfrac{\eta}{2\rho_0 c_s^3} \end{cases}. \tag{4}$$

$\omega = 2\pi f_0$ is the angular frequency. $\alpha_{0,p}$ and $\alpha_{0,s}$ are power law absorption factors.

For numerically solving the Kelvin-Voigt equation, the staggered-grid finite difference time domain (FDTD) method [8] combined with the perfectly matched layer (PML) [9] absorbing boundary is adopted.

2.2 Reconstruction of a 3D monkey skull

Figure 1 shows the reconstruction of the three-dimensional (3D) monkey skull. Usually, CT scans of the skull are used to reconstruct the 3D monkey skull.

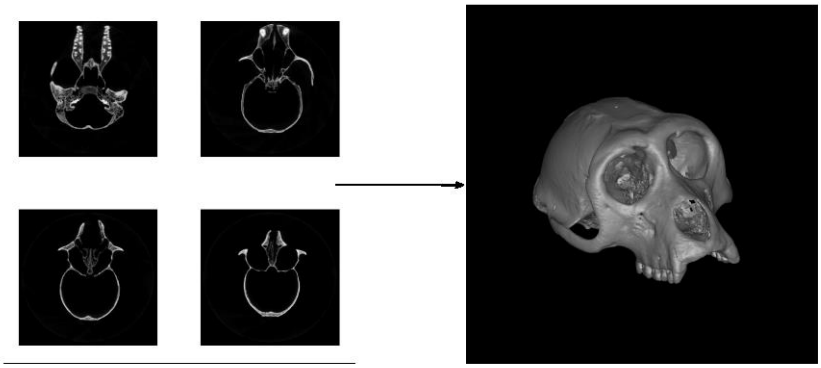

Figure 1: Reconstruction of a 3D monkey skull based on CT scans

To obtain acoustic parameters of the skull with strong heterogeneities, the relationship between the acoustic parameters and CT values of the skull [5] is employed.

$$\begin{cases} \phi = 1 - \dfrac{H}{1000} \\ \rho = \phi \times \rho_{skull,\min} + (1-\phi) \times \rho_{skull,\max} \\ c_p = \phi \times c_{p,skull,\min} + (1-\phi) \times c_{p,skull,\max} \\ \alpha_p = \alpha_{p,skull,\min} + \phi^{\gamma} \times \left(\alpha_{p,skull,\max} - \alpha_{p,skull,\min} \right) \end{cases}. \tag{5}$$

ρ is the density, c_p is the compressional wave velocity, and α_p is the compressional wave absorption coefficient. H, ϕ, $\rho_{skull,\min}$, $\rho_{skull,\max}$, $c_{p,skull,\min}$, $c_{p,skull,\max}$ and $\alpha_{p,skull,\min}$, $\alpha_{p,skull,\max}$ are the CT value, the porosity, the minimal and maximal densities, the minimal and maximal compressional wave velocities and the minimal and maximal compressional wave absorption coefficients of the skull, respectively. γ is commonly 0.5. The hypothetically precise acoustic parameters of the skull used in Eq. (5) are shown in Table 1.

Table 1: Hypothetically precise acoustic parameters employed in the simulation [10]

Sound velocity $(\mathrm{m/s})$		Acoustic absorption coefficient $(\mathrm{Np/m})$		Density $(\mathrm{kg/m^3})$	
$c_{p,skull,\min}$	1500	$\alpha_{p,skull,\min}$	7.37	$\rho_{skull,\min}$	1000
$c_{p,skull,\max}$	3100	$\alpha_{p,skull,\max}$	293.12	$\rho_{skull,\max}$	2200
c_{water}	1500	α_{water}	0.000288	ρ_{water}	1000

As for the shear wave velocity and the shear wave absorption coefficient of the skull, empirical formulas [10] are used, which can be expressed as:

$$\begin{cases} c_s = 4/7 \times c_p \\ \alpha_s = 90/85 \alpha_p \end{cases}. \tag{6}$$

where c_s and α_s are respectively the shear wave velocity and the shear wave absorption coefficient.

In order to analyse the effects of deviations of the monkey skull's density on transcranial focused ultrasound, a density deviation within the range -10%~+10% from the hypothetically precise density in Table 1 is updated to renew the reconstruction of the 3D monkey skull. And for the sound velocity and the absorption coefficient, the method for the density is followed. Furthermore, the acoustic parameters in Table 1 with the same deviation percentage are combined to renew the reconstruction of the 3D monkey skull for investigations.

2.3 Time-reversal method for precise transcranial focused ultrasound

The planar ultrasonic phased array transducer used for transcranial focused ultrasound is illustrated in Fig. 2. This array consists of 256 square elements distributed regularly in 16 rows and 16 columns with the same element size of $3.3\times3.3\text{mm}^2$ and the same kerf width of 0.2mm. The center frequency of the array is $f_0 = 0.8\text{MHz}$. The focusing location is 50mm in front of the array centre. Each element has a uniform emitting acoustic pressure amplitude p_0. For each element of the array, the acoustic pressure radiated is:

$$p_n = p_0 \sin\left(\omega t + \theta_{0n}\right). \tag{7}$$

The subscript n denotes the element number as shown in Fig. 2. θ_{0n} is the initial emitting phase of the nth element. In Eq. (2), the stress conditions for each element according to Eq. (7) become:

$$T_{ij} = -p\,\delta_n. \tag{8}$$

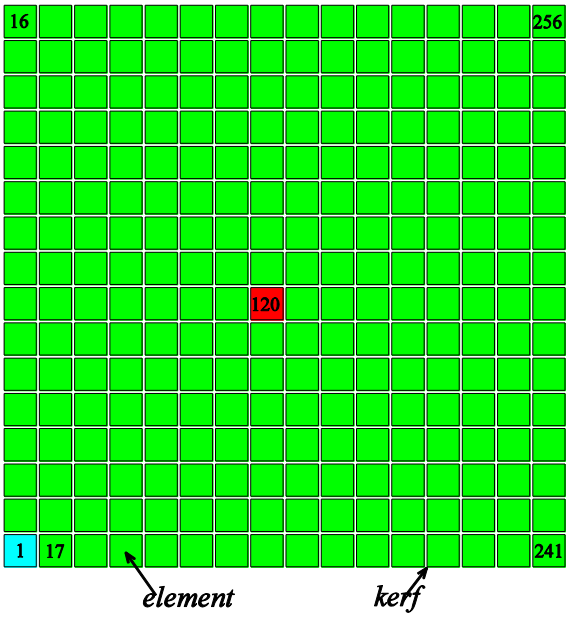

Figure 2: Schematic diagram of the planar ultrasonic phased array transducer

The skull is located between the array and the focus. Both the skull and the array are immersed in water. To precisely focus ultrasound through the skull at the focus, phase modulation based on the time-reversal method is necessary. For each 3D monkey skull model in Section 2.2, ultrasound

emitted from a virtual sinusoidal point source $p_{focus} = \sin(\omega t)$ at the focus is recorded by each element of the array. Then, the signal such as the normal stress T_{xx} received by an arbitrary element is chosen as reference set as $T_{xx,ref}$ and then undergoes self-correlation and cross-correlations with the received signals of any other elements to help calculate the initial emitting phase θ_{0n} for each element. Finally, all the transcranial focused ultrasound fields are simulated based on the hypothetically precise acoustic parameters of the skull, no matter by which 3D monkey skull model the initial emitting phase θ_{0n} is acquired.

3. Numerical results

Here, the focusing effect represented by the acoustic pressure focusing gain (p_f / p_0) and the focusing deviation ($\boldsymbol{r}_p - \boldsymbol{r}_t$) is employed to analyse the effects of deviations of the monkey skull's acoustic parameters on transcranial focused ultrasound, while the detailed distributions of transcranial focused ultrasound are not considered. p_f is the acoustic pressure amplitude at the practical focus, $\boldsymbol{r}_p$ is the practical focus location and $\boldsymbol{r}_t$ the theoretical focus location. The acoustic pressure focusing gain actually denotes the efficiency of the acoustic energy deposited at the focus by the array.

3.1 Acoustic pressure focusing gain dependent on deviation percentage from standard acoustic parameters

Figure 3 shows the acoustic pressure focusing gain dependent on the deviation percentage from the standard acoustic parameters, namely the hypothetically precise acoustic parameters. As can be seen from Fig. 3, in the scope of the deviation range of -10%~+10%, the deviations of the monkey skull's density and acoustic absorption coefficient have tiny effects on the acoustic pressure focusing gain of transcranial focused ultrasound. And the deviation of the sound velocity contributes major effects on the acoustic pressure focusing gain, since the curve of the acoustic pressure focusing gain dependent on the deviation percentage from the standard sound velocity generally coincides with the one of the acoustic pressure focusing gain dependent on the combined deviation percentage from the standard acoustic parameters. Additionally, the acoustic pressure focusing gain increases with the increase of the deviation percentage from the standard sound velocity, which indicates that an underestimation of the skull's sound velocity will lead to an underestimation of the acoustic pressure focusing gain and vise versa.

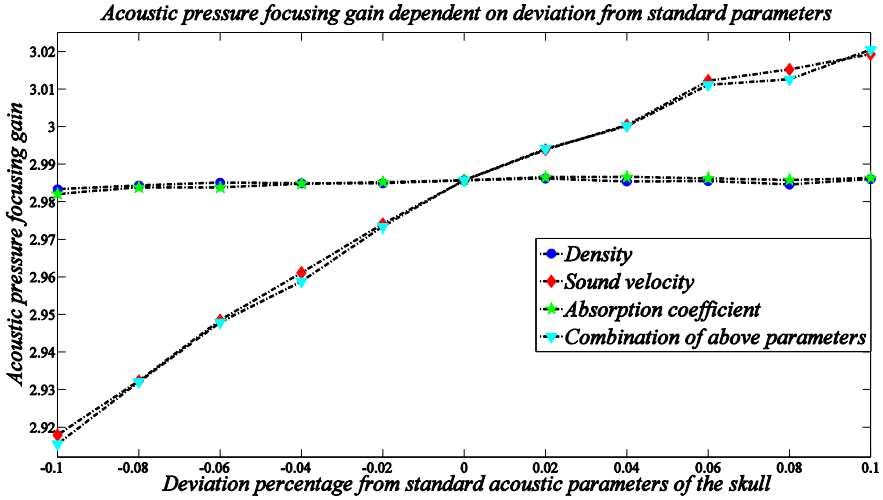

Figure 3: Acoustic pressure focusing gain of transcranial focused ultrasound dependent on the deviation percentage from standard acoustic parameters of the monkey skull

3.2 Focusing deviation dependent on deviation percentage from standard acoustic parameters

In Fig. 4, the focusing deviation dependent on the deviation percentage from the standard acoustic parameters is given. In the scope of the deviation percentage studied, we can see that the deviations of the monkey skull's density and acoustic absorption coefficient also have tiny effects on the focusing deviation of transcranial focused ultrasound. And the deviation of the sound velocity is also the major factor affecting the focusing deviation. Besides, the focusing deviation basically increases as the deviation percentage from the standard sound velocity increases. Actually, as long as the absolute deviation percentage from the standard sound velocity increases, the absolute focusing deviation increases. And an underestimation of the skull's sound velocity will make the practical focus location closer to the array, while an overestimation of the skull's sound velocity will make the practical focus location farther from the array. To control the absolute focusing deviation lower than 0.5mm (indicated by the red dotted line in Fig. 4), it is suggested that the absolute deviation percentage from the standard sound velocity should be less than 5.0%. According to Fig. 3, the deviation percentage threshold for the skull's sound velocity can ensure the deviation percentage of the acoustic pressure focusing gain less than approximately 1.0%, which is considered to be acceptable.

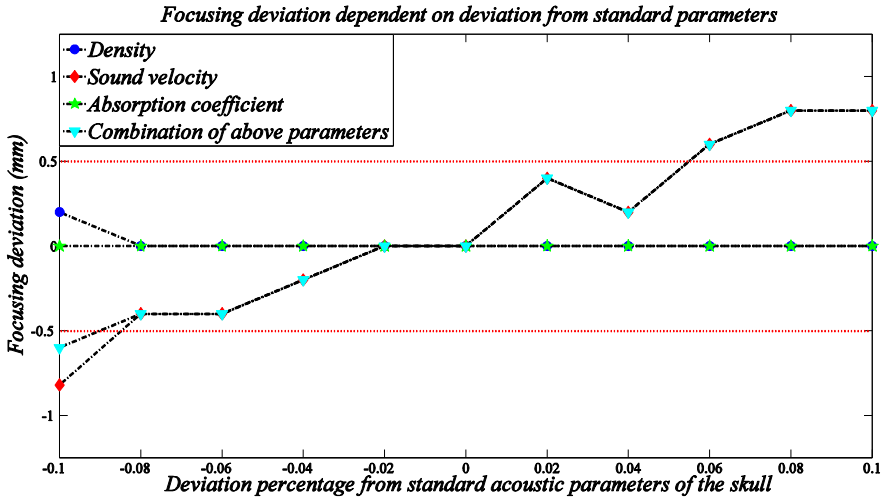

Figure 4: Focusing deviation of transcranial focused ultrasound dependent on the deviation percentage from standard acoustic parameters of the monkey skull

4. Conclusions

The effects of deviations of a monkey skull's acoustic parameters on transcranial focused ultrasound are investigated. A deviation percentage scope of -10%~+10% from the hypothetically precise acoustic parameters is chosen for the density, the sound velocity, the absorption coefficient and the combination of the above three parameters. By analysing the numerical results, we can see that both the acoustic pressure focusing gain and the focusing deviation representing the focusing effect of transcranial focused ultrasound are almost unaffected with the deviations of the monkey skull's density and acoustic absorption coefficient. The deviation of the sound velocity is the major factor influencing the acoustic pressure focusing gain and the focusing deviation. And, both the acoustic pressure focusing gain and the focusing increase with the increase of the deviation percentage from the standard sound velocity. Therefore, we propose based on the analysis that an absolute deviation percentage should be less than 5.0% from the standard sound velocity in order to keep the absolute focusing deviation lower than 0.5mm and the deviation percentage of the acoustic pressure focusing gain less than 1.0%.

ACKNOWLEDGEMENTS

This work is supported by the National Natural Science Foundation of China (Grant No. 11604361 and Grant No. 81527901).

REFERENCES

1 Jolesz, F. A., and McDannold, N. J. Magnetic Resonance–guided Focused Ultrasound: A New Technology for Clinical Neurosciences, *Neurologic Clinics*, 32(1): 253-269, (2014).

2 Colen, R. R., & Jolesz, F. A. Future Potential of MRI-guided Focused Ultrasound Brain Surgery, *Neuroimaging Clinics of North America*, 20(3): 355-366, (2010).

3 Pulkkinen, A., Werner, B., Martin, E., and Hynynen, K. Numerical Simulations of Clinical Focused Ultrasound Functional Neurosurgery, *Physics in Medicine and Biology*, 59(7): 1679, (2014).

4 White, P. J., Clement, G. T., and Hynynen, K. Longitudinal and Shear Mode Ultrasound Propagation in Human Skull Bone, *Ultrasound in Medicine & Biology*, 32(7): 1085-1096, (2006).

5 Aubry, J. F., Tanter, M., Pernot, M., Thomas, J. L., and Fink, M. Experimental Demonstration of Noninvasive Transskull Adaptive Focusing Based on Prior Computed Tomography Scans, *The Journal of the Acoustical Society of America*, 113(1): 84-93, (2003).

6 Mainardi, F. Fractional Calculus and Waves in Linear Viscoelasticity: An Introduction to Mathematical Models, *World Scientific*, (2010).

7 Fink, M. Time Reversal of Ultrasonic Fields. I. Basic Principles, *IEEE Transactions on Ultrasonics, Ferroelectrics, and Frequency Control*, 39(5): 555-566, (1992).

8 Graves, R. W. Simulating Seismic Wave Propagation in 3D Elastic Media Using Staggered-grid Finite Differences, *Bulletin of the Seismological Society of America*, 86(4): 1091-1106, (1996).

9 Berenger, J. P. A Perfectly Matched Layer for the Absorption of Electromagnetic Waves, *Journal of Computational Physics*, 114(2): 185-200, (1994).

10 Top, C. B., White, P. J., and McDannold, N. J. Nonthermal Ablation of Deep Brain Targets: A Simulation Study on a Large Animal Model, *Medical Physics*, 43(2): 870-882, (2016).